

Glial Swelling and Astrogliosis Produce Diffusion Barriers in the Rat Spinal Cord

EVA SYKOVÁ,* LÝDIA VARGOVÁ, ŠÁRKA PROKOPOVÁ, AND ZUZANA ŠIMONOVÁ
 Department of Neuroscience, 2nd Medical Faculty, Charles University, 150 18 Prague 5, Czech Republic, Department of Neuroscience, Institute of Experimental Medicine, Academy of Sciences of the Czech Republic, 142 20 Prague 4, Czech Republic

KEY WORDS anoxia; apparent diffusion coefficient; extracellular volume; glia; stroke; tortuosity

ABSTRACT Cell swelling and astrogliosis (manifested as an increase in GFAP) were evoked in isolated rat spinal cords of 4–21-day-old rats by incubation in either 50 mM K⁺ or hypotonic solution (235 mosmol kg⁻¹). Application of K⁺ and hypotonic solution resulted at first in a decrease of extracellular space (ECS) volume fraction α (ECS volume/total tissue volume) and an increase in tortuosity λ ($\lambda^2 = \text{free/apparent diffusion coefficient}$) in spinal gray (GM) and white matter (WM). These changes resulted from cell swelling, since the total water content (TW) in spinal cord was unchanged and the changes were blocked in Cl⁻-free solution and slowed down by furosemide and bumetanide. Diffusion in WM was anisotropic, i.e., more facilitated along fibers (x -axis) than across them (y - or z -axis). The increase of $\lambda_{y,z}$ was greater than that of λ_x , reaching unusually high values above 2.4. In GM only, during continuous 45 min application, α and λ started to return towards control values, apparently due to cell shrinkage of previously swollen cells since TW remained unchanged. This return was blocked by fluoroacetate, suggesting that most of the changes were due to the swelling of glia. A 45 min application of 50 mM K⁺ and, to a lesser degree, of hypotonic solution evoked astrogliosis, which persisted after washing out these solutions with physiological saline. During astrogliosis λ increased again to values as high as 2.0, while α either returned to or increased above control values. This persistent increase in λ after washout was also found in WM, and, in addition, the typical diffusion anisotropy was diminished. Our data show that glial swelling and astrogliosis are associated with a persistent increase in ECS diffusion barriers. This could lead to the impairment of the diffusion of neuroactive substances, extrasynaptic transmission, “crosstalk” between synapses and neuron-glia communication. *GLIA* 25:56–70, 1999. © 1999 Wiley-Liss, Inc.

INTRODUCTION

Changes in extracellular space (ECS) diffusion parameters may significantly affect communication between neurons as well as between neurons and glia. The diffusion of transmitters and other neuroactive substances through the ECS is also the underlying mechanism of extrasynaptic, or so-called “volume,” transmission in the brain (Fuxe and Agnati, 1991; Nicholson and Rice, 1991; Syková, 1992, 1997; Agnati et al., 1995; Barbour and Hausser, 1997; Nicholson and Syková, 1998). Any decrease in the ability of neuroactive sub-

stances, ions, or metabolites to diffuse through nervous tissue represents a serious clinical problem due to the potential for disrupting brain function (Andrew, 1991; Strange, 1992; Gullans and Verbalis, 1993). So far, it is not known whether astrocyte swelling, proliferation

Grant sponsor: GACR; Grant numbers: 309/96/0884, 307/96/K226, 309/97/K048, IGA MZ 3423–3.

*Correspondence to: Dr. Eva Syková, Department of Neuroscience, Institute of Experimental Medicine AS CR, Videňská 1083, 142 20 Prague 4, Czech Republic. E-mail: sykova@biomed.cas.cz

Received 16 March 1998; Accepted 8 May 1998

and hypertrophy during physiological and pathological states lead to persistent and functionally significant changes in ECS diffusion parameters.

Astrocyte swelling is an early event in numerous pathological states, such as ischemia, hyponatremia, and hepatic encephalopathy, and likely results from reduced extracellular osmolarity, elevated extracellular K^+ concentration, and/or glutamate (Kimelberg and Ransom, 1986; Kimelberg, 1991; Kimelberg et al., 1992; Hansson and Rönnbäck, 1994). When rapid cellular, particularly astrocytic, swelling occurs, water moves from the extra- to the intracellular compartment. This causes a decrease in ECS volume and changes in the geometry of the intercellular spaces (Syková, 1997; Nicholson and Syková, 1998), e.g., during repetitive neuronal activity (Ransom et al., 1985; Syková, 1987; Dietzel, et al., 1989; Svoboda and Syková, 1991), ischemia (Syková et al., 1994; Voříšek and Syková, 1997b), X-irradiation (Syková et al., 1996), and experimental autoimmune encephalomyelitis (Simonová et al., 1996). Several experimental conditions have been shown to result in ECS volume changes due to the movement of water from the extra- to the intracellular space. In particular, these include a decrease in the extracellular osmotic pressure (Andrew, 1991; Chebabo et al., 1995b; Križaj et al., 1996) and the accumulation of excitatory amino acids (Hansson and Rönnbäck, 1994; Syková et al., 1995). After the initial phase of swelling, cells, particularly astrocytes, actively down-regulate their volume by regulatory volume decrease (RVD) and by a net release of KCl, taurine, and other amino acids (Pasantes-Morales and Schousboe, 1988; Kimelberg, 1991; Pasantes-Morales et al., 1994); in this way, ECS volume can return to normal values. Even later, when glia become reactive, astrogliosis may result in the formation of additional and persistent diffusion barriers formed, for example, by the hypertrophy of fine glial processes or by an accumulation of macromolecules in the ECS (e.g., extracellular matrix proteins and cytokines) produced by neurons and glia (See Syková 1997).

By using the real-time iontophoretic method of diffusion analysis, the absolute values of ECS diffusion parameters and the time course of their changes can be determined in tissue for a substance of known size and structure, e.g., tetramethylammonium (TMA^+) (Nicholson and Phillips, 1981). Diffusion in the ECS is constrained by two factors. The first is the restricted volume of the selected tissue available for diffusing particles, i.e., the extracellular volume fraction α (ECS volume / total tissue volume). Second, the free diffusion coefficient, D , is reduced by the square of the tortuosity (λ) to an apparent diffusion coefficient $ADC = D/\lambda^2$, because in the CNS a diffusing substance encounters membrane obstructions, neuronal and glial processes, glycoproteins, and macromolecules of the extracellular matrix. In addition to these two geometrical constraints, the diffusion of many substances in the ECS is affected by nonspecific uptake, k' , a factor describing the loss of a substance across cell membranes (Nicholson and Phillips, 1981). The TMA^+ -method is the most

versatile and convenient method for studying ECS diffusion parameters since it can measure absolute values of α , λ , k' and ADC simultaneously. Water redistribution in the brain during various physiological and pathological states can also be studied by other methods, namely, by intrinsic optical signals and light scattering in brain slices (Lipton, 1973; MacVicar and Hochman, 1991; Andrew and MacVicar, 1994; Holthoff and Witte, 1996) and in vivo by diffusion-weighted magnetic resonance imaging (DW-MRI) (Benveniste et al., 1992; Latour et al., 1994; Norris et al., 1994; Van der Toorn et al., 1996). These methods are less complete for studies of ECS diffusion parameters since they do not allow one to determine the absolute values and time course of all three diffusion parameters or to study diffusion heterogeneity and anisotropy.

In the present study, we examined changes in the ECS diffusion parameters α , λ , k' , and ADC evoked by elevated K^+ or hypotonic stress in isolated rat spinal cord. The changes evoked by acute cell swelling were compared with those seen during astrogliosis, here manifested as an increase in glial fibrillary acidic protein (GFAP) staining. The isolated spinal cord has been shown to behave in a similar manner as an in vivo preparation (Prokopová et al., 1997), with the advantage that drugs can be applied in a superfusing solution and measurements are not affected by systemic side effects. TMA^+ diffusion profiles were analyzed in gray and white matter of rats 4–21 days old, i.e., in the period prior to and during extensive gliogenesis and myelination. We asked the questions whether the same mechanisms that are involved in cell swelling are also involved in both ECS volume fraction decrease and tortuosity increase, and whether the two diffusion parameters may change independently of one another. We found that astrogliosis results in the formation of persistent diffusion barriers. By this mechanism glial cells could significantly affect neuronal excitability, synaptic as well as extrasynaptic transmission and be involved in plastic changes.

MATERIALS AND METHODS

Animal Preparation and Solutions

All animals were Wistar rat pups divided into groups according to their age: P4–5, P10–13, and P20–21, where P indicates postnatal age in days. Following decapitation under ether anesthesia, spinal cords were isolated in a chamber with cold (8°C) artificial cerebrospinal fluid (ACF) of the following composition (in mM): NaCl 117.0, KCl 3.0, $NaHCO_3$ 35.0, Na_2HPO_4 1.25, D-glucose 10.0, Sodium Ascorbate 0.2, Thiourea 0.2, $MgCl_2$ 1.3, and $CaCl_2$ 1.5. The solution was saturated with 95% O_2 and 5% CO_2 (pH about 7.3). The isolated spinal cord was placed in a small chamber, and the preparation was continuously perfused with ACF containing 0.1 mM of tetramethylammonium chloride at a rate of 10 ml/min. During about 1 h the temperature was increased to 21–22°C.

Hypoosmotic solutions were prepared by reducing the NaCl content of the ACF. The osmotic strength of the solutions was measured with a vapor pressure osmometer. Thus "normal" ACF had an osmolarity of 300 mmol kg⁻¹, H-40 of 235 mmol kg⁻¹, and H-80 of 149 mmol kg⁻¹. Solutions with an increased K⁺ or Mg⁺⁺ concentration had a reciprocally reduced Na⁺ concentration. Ca⁺⁺-free solutions were prepared by omitting CaCl₂ and adding 1 mM EGTA (Sigma Chemical Co., St. Louis, MO). In Cl⁻-free solutions, NaCl was replaced with Na-gluconate, KCl with K-gluconate, CaCl₂ with Ca(CH₃COO)₂, and MgCl₂ with MgSO₄ in equimolar amounts. All drugs were dissolved and applied to the spinal cord in ACF. We used 5 mM BaCl₂, 2 mM furosemide, 0.1 mM bumetanide, and 0.1 mM fluoracetate-Na⁺ (all from Sigma Chemical Co., St. Louis, MO).

Measurements of Extracellular Space Diffusion Parameters

To estimate diffusion parameters in the extracellular space (ECS), the real-time iontophoretic method originally developed by Nicholson and Phillips (1981) and described in our previous studies (Lehmenkühler et al., 1993; Syková et al., 1994) was used. In brief, an extracellular marker such as tetramethylammonium ions (TMA⁺), to which cell membranes are relatively impermeable, is administered into the tissue by iontophoresis. The concentration of TMA⁺ measured in the ECS by a TMA⁺-selective microelectrode (ISM) is inversely proportional to the ECS volume. Double-barreled TMA⁺-ISMs were prepared by the procedure described in Syková (1992). The liquid ion-exchanger was Corning 477317 (Rochester, NY), which is highly sensitive to TMA⁺, and the TMA⁺-sensitive barrel was backfilled with 100 mM TMA chloride. The reference barrel contained 150 mM NaCl. The TMA⁺-ISMs were calibrated in 0.01, 0.03, 0.1, 0.3, 1.0, 3.0, and 10.0 mM TMA⁺ in a background of either 3 or 50 mM KCl and 150 or 103 mM NaCl. Calibration data were fitted to the Nikolsky equation to determine electrode slope and interference. The electrode slope was equal in both 3 and 50 mM KCl backgrounds.

Iontophoretic micropipettes were made from theta glass. The shank was bent so that it could be aligned parallel to the TMA⁺-ISM and filled with 100 mM TMA⁺. To stabilize the intertip distance (100–180 μm), both electrodes were glued together with dental cement. Typical iontophoresis parameters were +20 nA bias current (continuously applied to maintain a constant transport number) with an +80 nA current step of 60 s duration to generate the diffusion curve. TMA⁺ diffusion curves were captured on a digital oscilloscope (Nicolet 3091) and then transferred to a PC-compatible 486 computer, where they were analyzed by fitting the data to a solution of Eq. [1] (Nicholson and Phillips, 1981), by using the program VOLTORO (Nicholson, unpublished).

TMA⁺ diffusion curves were first recorded in 0.3% agar gel (Difco, Detroit, MI, Special Noble Agar) made up in 150 mM NaCl, 3 mM KCl, and 1 mM TMA⁺. The

electrode array was then lowered into an isolated spinal cord to a depth of 250–350 μm from the dorsal spinal surface. Diffusion measurements in gray matter were only done along one axis (perpendicular to the long spinal cord axis) since diffusion is isotropic in spinal cord dorsal horn gray matter (Prokopová et al., 1997). The location of the ISM in white matter was determined from the ventral horn spinal surface, and recordings were done at a depth of about 300 μm. Since diffusion in myelinated spinal cord white matter is anisotropic (with one λ value in the *x*- and another in the *y*- and *z*- axes), measurements were performed along two perpendicular axes, the *x*-axis being along the spinal cord axis (i.e., along the axons) and the *y*-axis being perpendicular to the *x*-axis (i.e., across the axons) (Prokopová et al., 1997). The diffusion curves obtained from the spinal cord were then analyzed to yield *a*, λ, and *k*. These three parameters were extracted by a nonlinear curve-fitting simplex algorithm operating on the diffusion curve described by Eq. [1], which represents the behavior of TMA⁺, assuming that it spreads out with spherical symmetry, when the iontophoresis current is applied for duration *S*. In this expression, *C* is the concentration of the ion at time *t* and distance *r* (distance from the source electrode). The equation governing diffusion in nervous tissue is:

$$C = G(t) \quad t < S, \text{ for the rising phase of the curve}$$

$$C = G(t) - G(t - S) \quad t > S, \text{ for the falling phase of the curve}$$

The function *G(u)* is evaluated by substituting *t* or *t-S* for *u* in the following equation:

$$G(u) = (Q\lambda^2/8\pi D\alpha r) \{ \exp [r\lambda(k'/D)^{1/2}] \operatorname{erfc} [r\lambda/2(Du)^{1/2} + (k'u)^{1/2}] + \exp [-r\lambda(k'/D)^{1/2}] \operatorname{erfc} [r\lambda/2(Du)^{1/2} - (k'u)^{1/2}] \} \quad (1)$$

The quantity of TMA⁺ delivered to the tissue per second is *Q* = *In*/*zF*, where *I* is the step increase in current applied to the iontophoresis electrode, *n* is the transport number, *z* is the number of charges associated with the substance iontophored (+1 here), and *F* is Faraday's electrochemical equivalent. The function "erfc" is the complementary error function. In agar α and λ are by definition set to 1 and *k*' is set to 0; the parameters *n* and *D* are extracted by curve fitting. Knowing *n* and *D*, the parameters α, λ, and *k*' can be obtained when the experiment is repeated in spinal cord.

By using the TMA⁺ method, anisotropic diffusion was found in cerebellum (Rice et al., 1993), in myelinated corpus callosum (Chvátal et al., 1997; Voříšek and Syková, 1997a) and in spinal cord myelinated white matter (Prokopová et al., 1997). Diffusion is facilitated along the axons (*x*-axis) of the ventral funiculus and hindered across the axons (*y*- and *z*-axis), i.e., the value of λ is higher. We therefore determined the true value of α in white matter from the relation α = (λ_yλ_z/λ_x²)α_x (for

details see Rice et al., 1993; Voříšek and Syková, 1997a). For this calculation, we assumed diffusion to be equal along both axes lying at right angles to the direction of the axons, i.e., the *y*- and *z*-axes (see Prokopová et al., 1997).

Determination of Total Tissue Water

The total tissue water content was determined in freshly isolated spinal cords, isolated spinal cords incubated for 45 min at 21–22°C in either ACF, hypotonic solution (H-40), or ACF with 50 mM K⁺, and isolated spinal cords incubated for 45 min in 50 mM K⁺ and then 60 min in ACF. After incubation spinal cords were blotted to remove excess saline and then weighed to yield wet weight (WW), then dried at 80–90°C until they reached a constant weight (dry weight, DW). If we assume that the tissue comprises three compartments, extracellular water, intracellular water, and dry solids (which stay constant during drying), the total percentage of water (TW) can be calculated as the difference between dry and wet weight according to formula:

$$TW (\%) = (WW - DW) / WW \times 100.$$

Immunohistochemistry

Immunohistochemical and morphological studies were undertaken on the 21 spinal cords which were incubated in either ACF, ACF with 50 mM K⁺, or H-40. As controls, spinal cords from other pups of the same litters were isolated and processed simultaneously. In all cases, spinal cords were fixed with 4% paraformaldehyde in 0.1 M phosphate-buffered saline (PBS; pH 7.5) for 4 h, trimmed, and then immersed in PBS containing 30% sucrose. Frozen transverse and longitudinal sections (40 μm) were cut through the lumbar part of the spinal cord. Selected sections were immunostained or stained with cresyl violet (Nissl). Astrocytes were identified using monoclonal antibodies to GFAP (Boehringer-Mannheim, Mannheim, Germany); oligodendrocytes and myelin were immunostained with Rip, a monoclonal antibody specific for oligodendroglia and central myelin obtained from the Developmental Studies Hybridoma Bank, Iowa City, IA (Friedman et al., 1989). GFAP antibodies were diluted to 0.4 μg/ml in PBS containing 1% bovine serum albumin (BSA, Sigma Chemical Co., St. Louis, MO) and 0.2% Triton X-100. The partially purified Rip supernatant was diluted 1:50 in PBS with 1% BSA and 0.2% Triton X-100 added. Immunostaining for chondroitin sulfate proteoglycans was done using CS-56 antibody (Sigma Chemical Co., St. Louis, MO) diluted 1:500 in PBS with 1% BSA and 0.2% Triton X-100 added (Harvey et al., 1997). After overnight incubation in the primary antibodies at 4°C, the floating sections were washed and processed by using biotinylated anti-mouse secondary antibodies and the peroxidase-labeled avidin-biotin complex method (Vectastain Elite, Vector Laboratories, Burlin-

game, CA). Immune complexes were visualized using 0.05% 3,3'-diaminobenzidine tetrachloride (Sigma Chemical Co., St. Louis, MO) in PBS and 0.02% H₂O₂.

RESULTS

Total Water Content in Isolated Rat Spinal Cord: Effects of elevated K⁺ and hypotonic stress

The effects of elevated K⁺ concentration and hypotonic stress on the total water content of the isolated spinal cord were studied in order to determine whether, after such a procedure, the water content of the tissue actually increases or whether water only shifts from the extra- to the intracellular compartment. Measurements of total water content (Table 1) revealed that the percentage of water in the freshly isolated rat spinal cord was higher at P10 than at P20 and significantly higher still at P4–5. Importantly however, at all three ages the water content in freshly isolated spinal cords was not significantly different from that in isolated spinal cords incubated for 45 min, or even 2 h, in physiological ACF (Table 1).

In all three age groups studied (P4–5, P10, and P20), the total water content in spinal cords incubated for 45 min in ACF with 50 mM K⁺ was not significantly different from that seen in spinal cords incubated in physiological ACF, i.e., with 3 mM K⁺. Similarly, when spinal cords were first superfused for 45 min with 50 mM K⁺ and then 60 min with ACF (total incubation time 2 h), the water content was not significantly different from that following a 2 h incubation in ACF (Table 1). These results show that after potassium application, the total amount of water did not increase; therefore, the observed changes in extracellular space volume (see below) were due to a shift of water from the extra- to the intracellular compartment only.

The total water content in spinal cords incubated for 45 min in hypotonic solution (H-40) was higher, by about 2%, than that in spinal cords incubated in ACF (Table 1). Cross-sectional measurements of spinal cord diameter, made in the lumbar region of three animals at P10, revealed that after a 45 min incubation in H-40 the spinal cord diameter increased from 1.75, 1.8, and 1.9 mm (incubation in ACF prior to H-40) to 1.9, 2.0, and 2.1 mm, i.e., by about 10–15% (see also Fig. 8A,B). The observed ECS volume decrease in a hypoosmotic solution might therefore be partly affected by the tissue's gaining water and not only by a shift of water between the extra- and intracellular compartments.

Effect of Elevated K⁺ Concentration on Diffusion Parameters in Dorsal Horn Gray Matter

A transient increase in extracellular K⁺ concentration in the range of 6–50 mM accompanies physiological stimulation and many pathological states, depending on the developmental stage and CNS region (for review see Syková, 1983, 1992). Therefore, the effect of 10, 20,

TABLE 1. Percentage of water in the isolated spinal cord and after incubation in artificial cerebrospinal fluid (ACF), ACF with 50 mM K⁺ or hypotonic solutions^a

Age	Freshly isolated spinal cord	Incubation in ACF (45 min)	Incubation in 50 mM K ⁺ (45 min)	Incubation in H-40 (45 min)	Incubation in ACF (105 min)	Incubation in 50 mM K ⁺ (45 min) and in ACF (60 min)
P4–5	85.42 ± 0.30 (n = 6)	84.89 ± 0.31 (n = 11)	84.81 ± 0.26 (n = 6)	86.33 ± 0.29*	—	—
P10	84.03 ± 0.17# (n = 6)	84.52 ± 0.22 (n = 6)	84.97 ± 0.40 (n = 7)	85.99 ± 0.53**	84.61 ± 0.22 (n = 5)	84.87 ± 0.22 (n = 5)
P20	79.43 ± 0.48## (n = 6)	80.27 ± 0.48## (n = 6)	79.25 ± 0.20## (n = 6)	—	—	—

^aThe percentage of water is expressed as mean ± S.E.M., n is the number of animals. Prior to incubation in ACF, 50 mM K⁺ or H-40, all spinal cords were incubated for at least 25 min in ACF. Statistical analysis of the differences between control (incubation in ACF) and incubation in 50 mM K⁺ or hypotonic solutions was performed by one-way ANOVA test: **P* < 0.05, ***P* < 0.01. The differences between age groups (P10 was compared to P4–5 and P20 to P10): #*P* < 0.005, ##*P* < 0.0001.

or 50 mM K⁺ on ECS diffusion parameters was tested in three age groups: P4–5, P10–13, and P20–21. In all age groups an increase from 3 to 10 mM K⁺ did not result in a significant change in α , and in 20 mM K⁺ a relatively small decrease in α was found (e.g., from 0.23 to 0.21), while λ was clearly increased in 10 mM K⁺ (e.g., from 1.61–1.63 to 1.72–1.73) and even more in 20 mM K⁺ (e.g., from 1.61 to 1.82) (see Fig. 1).

The application of 50 mM K⁺ led to dramatic changes in both α and λ (Fig. 1, Table 2). A 45 min superfusion of isolated spinal cord with an isotonic solution containing 50 mM K⁺ led at first to a decrease in α and an increase in λ in all age groups (Table 2, Fig. 2), the so-called Phase I (Fig. 3A,B). In dorsal horn gray matter α decreased to 0.07 at P4–P5, to 0.09 at P10–13 and to 0.17 at P20–21, while λ increased to about 2.06 at P4–5, 2.16 at P10–13, and 1.93 at P20–21. Figure 3A,B further shows that Phase I was significantly longer (25–30 min) at P4–P5 than at P10–P13 (5–10 min) or at P20–21 (< 5 min, not shown). When the application of 50 mM K⁺ continued after this time, α , particularly in animals at P10 and older, started to increase, i.e., to return towards control values, here called Phase II (Fig. 3B). Since the total water content remained unchanged during Phase II (Table 1), it is evident that water shifted from the intra- to the extracellular compartment, i.e., from swollen cells back to the interstitial space. The observed recovery of α in 50 mM K⁺ might therefore be due to regulation of the cell volume, i.e., regulatory volume decrease (RVD). It is important to notice, however, that at the same time λ either remained elevated or even increased further (Figs. 2, 3B). This Phase II started much later at P4–5 than at P10–13 (Fig. 3A,B) or P20–21 (not shown). At P20–21, Phase I was so short that the first diffusion curve captured 5 min after the application of 50 mM K⁺ already revealed, in four experiments out of six, an increase in α due to RVD, which was accompanied by a typical increase in λ . The mean decrease in α values, as recorded 5 min after the application of 50 mM K⁺ and as shown in Table 2, is therefore only marginally significant.

When the spinal cords were again superfused with 3 mM K⁺ ACF, α continued to quickly increase towards control values, while λ decreased only partially, by about 80% at P4–5 and about 50% at P10 and older (Figs. 2, 3A,B). After this recovery phase, here called Phase III, α rose above control values by about 100% in animals at P10 and older, reaching values of 0.35–0.45

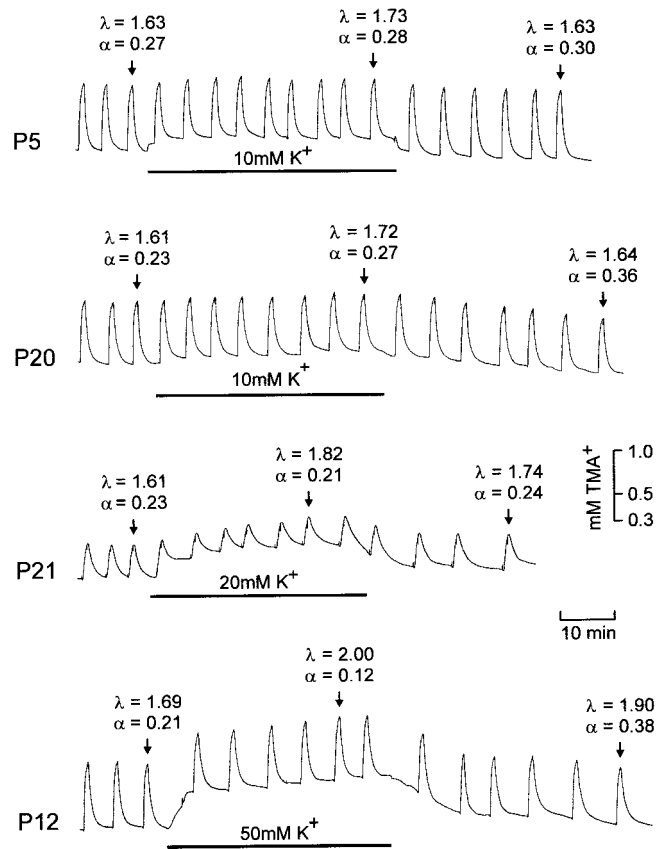


Fig. 1. Representative recordings of tetramethylammonium (TMA⁺) diffusion curves in spinal cord dorsal horn at different postnatal days during the application of 10, 20, or 50 mM K⁺. The effect of 10 mM K⁺ is shown in 5- and 20-day-old animals (P5, P20), 20 mM K⁺ at P21 and 50 mM K⁺ at P12. Diffusion curves are superimposed on an increasing TMA⁺ baseline. Values of ECS volume fraction (α) and tortuosity (λ) are shown with three diffusion curves: prior to, during, and after the application of increased potassium. Note that the amplitudes of the diffusion curves are not inversely proportional to the size of the ECS volume fraction, because they are superimposed on different TMA⁺ baselines.

(Phase IV). This Phase IV, an increase in the volume of the extracellular space above physiological values (ECS overshoot), was accompanied by a second increase in λ values to as high as 1.8–2.0 (Fig. 3B). The changes in α and λ persisted even 100 min after the application of 50 mM K⁺. These results show that in more mature animals, which have been shown to have a smaller ECS (see Table 2) as a result of more advanced gliogenesis (Prokopová et al., 1997), the cells exposed to high K⁺

TABLE 2. The values of α , λ , and k' during a 45 min application of 50 mM K^+ or hypotonic solutions in the GM and WM of the isolated spinal cord^a

Age	ACF	50 mM K^+	H-40	H-80
GM P4-5	$\alpha = 0.25 \pm 0.01$ $\lambda = 1.53 \pm 0.02$ $k' = 7.18 \pm 0.83$ (n = 20)	$\alpha = 0.07 \pm 0.01^{***}$ $\lambda = 2.06 \pm 0.06^{***}$ $k' = 2.13 \pm 0.84^{**}$ (n = 8)	$\alpha = 0.15 \pm 0.01^{***}$ $\lambda = 1.62 \pm 0.02^*$ $k' = 5.85 \pm 0.41$ (n = 7)	$\alpha = 0.11 \pm 0.02^{***}$ $\lambda = 1.72 \pm 0.07^{**}$ $k' = 4.25 \pm 2.27$ (n = 5)
GM P10-13	$\alpha = 0.22 \pm 0.01\#$ $\lambda = 1.60 \pm 0.01\#\#$ $k' = 5.25 \pm 0.50\#$ (n = 25)	$\alpha = 0.09 \pm 0.01^{***}$ $\lambda = 2.16 \pm 0.06^{***}$ $k' = 5.21 \pm 0.94\#$ (n = 14)	$\alpha = 0.13 \pm 0.01^{***}$ $\lambda = 1.83 \pm 0.06^{***}\#\#$ $k' = 2.38 \pm 0.89^*\#\#$ (n = 6)	$\alpha = 0.08 \pm 0.01^{***}$ $\lambda = 1.93 \pm 0.01^{***}\#\#$ $k' = 2.21 \pm 0.63^*$ (n = 5)
GM P20-21	$\alpha = 0.21 \pm 0.01\#$ $\lambda = 1.62 \pm 0.02\#$ $k' = 3.05 \pm 0.36\#\#$ (n = 12)	$\alpha = 0.17 \pm 0.02$ m.s.### $\lambda = 1.93 \pm 0.09^{***}$ $k' = 3.78 \pm 0.80$ (n = 6)	$\alpha = 0.11 \pm 0.01^{***}\#\#$ $\lambda = 1.79 \pm 0.02^{***}\#\#\#$ $k' = 2.75 \pm 0.98\#$ (n = 6)	—
WM P13-14	$\alpha = 0.23 \pm 0.01$ $\lambda_x = 1.38 \pm 0.01$ (n = 15) $\lambda_y = 1.82 \pm 0.01$ (n = 11) $k' = 7.06 \pm 0.39$	$\alpha = 0.12 \pm 0.01^{***}$ $\lambda_x = 1.92 \pm 0.07^{***}$ (n = 9) $\lambda_y = 2.42 \pm 0.05^{***}$ (n = 5) $k' = 3.30 \pm 0.59^{***}$	$\alpha = 0.10 \pm 0.01^{***}$ $\lambda_x = 1.83 \pm 0.05^{***}$ (n = 6) $\lambda_y = 2.00 \pm 0.07^{**}$ (n = 6) $k' = 2.26 \pm 0.68^{***}$	—

^aThe values for extracellular volume fraction α (mean \pm S.E.M., n is the number of animals), tortuosity λ , and non-specific uptake k' ($\times 10^{-3} s^{-1}$) represent the stable values in ACF or maximal changes evoked by the application of 50 mM K^+ or hypotonic solutions. λ_x and λ_y represent measurements along the axons (x-axis) and across the axons (y-axis). Statistical significance was evaluated as the difference between controls (ACF) and the values during application, using one-way ANOVA test: m.s. (marginally significant), * $P < 0.05$, ** $P < 0.005$, *** $P < 0.0005$; and as the difference between P4-5 and P10-13 or P20-21 in the gray matter: # $P < 0.05$, ## $P < 0.005$, ### $P < 0.0005$.

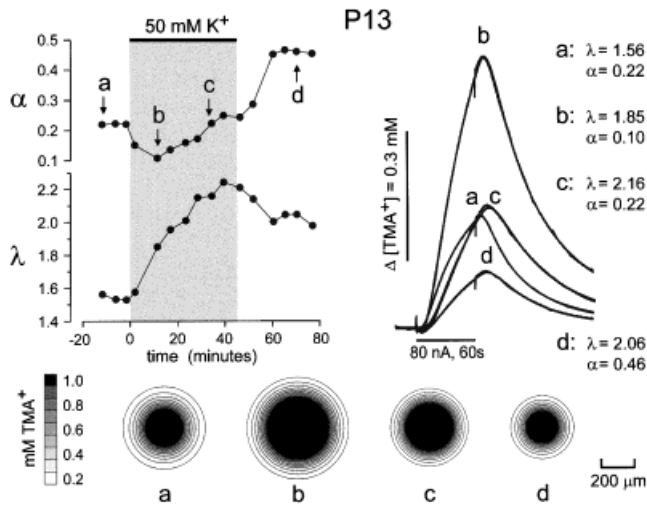


Fig. 2. A typical effect of 50 mM K^+ in a 13-day-old animal (P13). The time course of changes is shown at the upper left. The normalized diffusion curves obtained at points a, b, c, and d and the corresponding values of α and λ are shown at the upper right. Note that the amplitudes of the normalized diffusion curves are inversely proportional to the size of the ECS volume fraction. By using the values obtained at points a, b, c, and d, two-dimensional isoconcentration plots of extracellular TMA^+ concentration were constructed (a, b, c, and d). Gray densities represent the concentration of TMA^+ , from 0.2 to 1.0 mM, reached 60 s after the onset of an 80 nA iontophoretic pulse (bottom of the figure). The radius of the circles is inversely proportional to the size of the ECS volume fraction; the pattern of changes in TMA^+ concentration reflects the tortuosity.

may more effectively regulate their volume. Only at P4-5 did nonspecific TMA^+ uptake (k') decrease during the application of elevated K^+ (Table 2).

The diffusion of a neuroactive substance is modified by both diffusion parameters, α and λ . The changing values of α and λ obtained in one experiment were therefore used to construct isoconcentration plots in the x - y plane representing diffusion in the spinal cord. The

circles in Figure 2 illustrate the concentration of TMA^+ (0.2–1.0 mM) as calculated 60 s after its iontophoretic application in a P13 animal. Isoconcentration circles in the spinal cord during the application of 50 mM K^+ (see Fig. 2, circle b) are significantly larger than those recorded prior to its application, i.e., in 3 mM K^+ (Fig. 2, circle a). Thus, during the application of high K^+ , the area in which TMA^+ concentration reaches any given level (0.2–1.0 mM) is significantly larger than the area reaching the same level in 3 mM K^+ (primarily because of the smaller ECS volume). Figure 2 further shows that during Phase II, when α returns toward control values but λ reaches its highest values, the circles representing the highest TMA^+ concentrations (0.6–1.0) are larger than in controls (Fig. 2, circle c). However, following the application of high K^+ , when the spinal cord is again perfused with ACF and the ECS volume is more than doubled as compared to control values, the isoconcentration circles at any given concentration are smaller than those in control tissue (Fig. 2, circle d). The isoconcentration plots show that the diffusion of TMA^+ depends on both diffusion parameters, α and λ ; it is hindered during elevated K^+ (Phase I) but later, during recovery in ACF, is actually facilitated.

In about 10% of the experiments (n = 8), the application of 50 mM K^+ led to a decrease in α to 0.05–0.07 and an increase in λ to 1.9–2.0; however, there was no recovery towards control values when the spinal cord was again perfused with 3 mM K^+ ACF, i.e., there was no Phase II, III, or IV.

Effect of Hypotonic Stress on ECS Diffusion Parameters in Gray Matter

The effect of two hypotonic solutions (H-40 and H-80) was tested on three animal age groups, P4-5, P10-13,

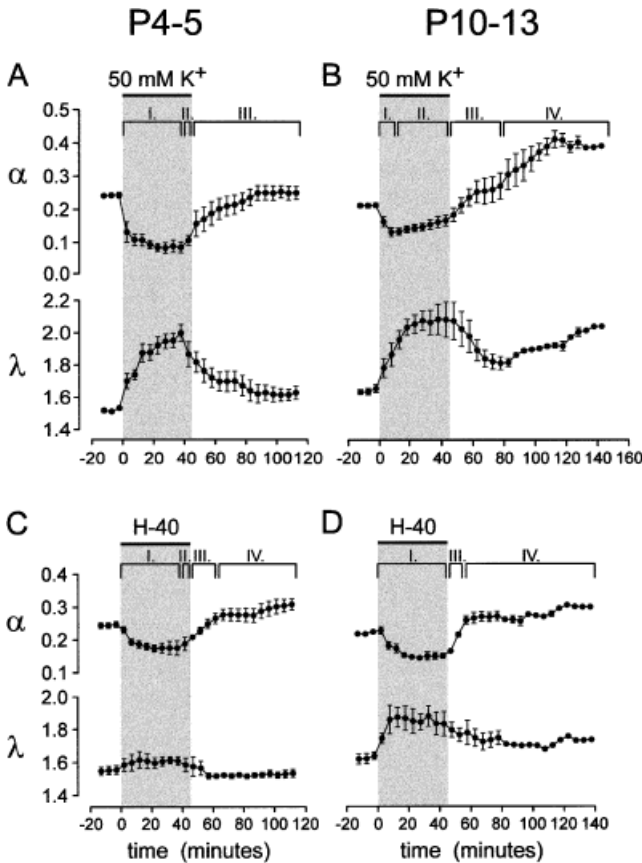


Fig. 3. The effect of 50 mM K^+ (A,B) and hypotonic solution H-40 (235 mosmol kg^{-1}) (C,D) on ECS diffusion parameters in gray matter as measured in two age groups, P4–5 and P10–13. Each data point represents mean \pm S.E.M., calculated from α and λ values recorded at 5 min intervals from 4 (A and D) or 7 (B and C) experiments. The changes were divided into four phases: Phase I: Application-evoked decrease of α and increase of λ . Phase II: During application, α returned towards control values, possibly due to regulatory volume decrease (RVD), while λ either remained unchanged or increased further. Phase III: During washout of 50 mM K^+ or hypotonic solution with isotonic, 3 mM K^+ artificial cerebrospinal fluid (ACF), α overshoot control values and λ partially decreased towards control values. Phase IV: In ACF α remained elevated, overshooting control values, but λ showed a second increase. Note: Phase I was slower at P4–5 than at P10–13. Phase II in 50 mM K^+ was more pronounced at P10–13 than at P4–5 and it was more pronounced than in hypotonic solutions. Phase IV was absent at P4–5 following 50 mM K^+ .

and P20–21, to compare the effect of hypotonic swelling with that of K^+ -evoked cell swelling on ECS diffusion parameters. The application of hypotonic solutions for 45 min resulted in a gradual decrease in α and an increase in λ in dorsal horns (Fig. 3C,D; Phase I). A comparison of the three age groups showed that in contrast to 50 mM K^+ , the decrease in α evoked by H-40 was not significantly different at P20–21, P10–13, or P4–5, while the increase in λ was significantly larger at P10–13 and P20–21 than at P4–5 (Fig. 3C,D; Table 2). In contrast to 50 mM K^+ , the time course of the changes was not significantly different between the groups (Fig. 3C,D). In two of six experiments at P20–21, three of six at P10–13, and three of seven at P4–5, α started to increase after about 30 min or 40 min of H-40 application, respectively; however, unlike the increase in α seen during the application of 50 mM K^+ , this increase was not significant (Phase II was short or absent; Fig.

3C,D). Nonetheless, after recovery in isoosmotic solution, α quickly returned to its original value in all age groups (Phase III), and then overshoot control values by about 50%, reaching values of 0.30 (Phase IV; Fig. 3C,D). In the two older age groups only, λ increased to about 1.75 while α remained increased, but even this persistent increase in λ was significantly smaller than the increase in λ following the application of 50 mM K^+ (compare Phase IV in Fig. 3B,D).

The application of H-80 resulted in a larger decrease in α than did that of H-40 (Table 2); α remained decreased and λ remained increased throughout the 45 min application, i.e., there was no sign of recovery. However, the increase in λ was still significantly smaller than that in 50 mM K^+ . After recovery of spinal cords to isotonic ACF, α at P4–5 returned to control values, followed by a relatively small overshoot of 10–15% above control values, but the recovery of λ was incomplete. At P10–13, no recovery of α or λ was seen in isotonic ACF, as was also the case in some experiments following the application of 50 mM K^+ . This suggests that in older animals, H-80 evoked irreversible cell swelling, and presumably also cell damage, accompanied by a decrease in ECS volume and an increase in tortuosity.

Effects of Elevated K^+ and Hypotonic Stress in White Matter

In animals at P13–14, i.e., after advanced spinal cord myelination, the effect of 50 mM K^+ and H-40 was studied in spinal cord white matter (ventral funiculus), approached by microelectrodes from the ventral spinal cord surface. Since diffusion in myelinated white matter at P13–14 is anisotropic (Prokopová et al., 1997) with only two different values of tortuosity (λ_x and $\lambda_{y,z}$), we performed measurements in two axes (x and y , along and across the myelinated axons). Table 2 and Figure 4 demonstrate that in white matter, the application of 50 mM K^+ or H-40 resulted in a similar decrease in α and increase in λ_x . However, a much greater increase in λ_y (across the axons) was observed during the application of 50 mM K^+ , reaching unusually high values of 2.42 (higher than that observed in gray matter). On the contrary, in H-40, after an initial small increase, λ_y significantly decreased and both λ_x and λ_y reached similar values of about 1.8. This loss of anisotropy persisted even during the application of isotonic ACF. A loss of anisotropy was also found after the application of 50 mM K^+ when the spinal cord was superfused with 3 mM K^+ ACF. No Phase II (a return of α towards control values during application) or Phase IV (an overshoot of α control values by more than 5%) were observed in white matter (Fig. 4). The isoconcentration ellipses in Figure 4a,b,d, and e, as calculated 60 s after TMA⁺ iontophoretic application, demonstrate the existence of anisotropic diffusion prior to and during the application of 50 mM K^+ and, initially, also H-40. Both applications, 50 mM K^+ and H-40, resulted in changes in λ_x and λ_y that persisted for more than 40 min after the return to ACF; the isoconcentration circles, replacing the ellipses, show the disappearance of diffusional anisotropy (Fig. 4c,f).

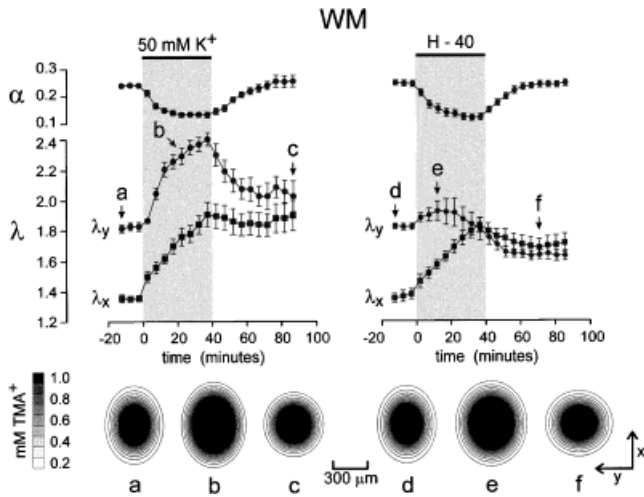


Fig. 4. The effect of 50 mM K^+ and H-40 in white matter (WM) of 10–13-day-old rats. As diffusion in WM is anisotropic (with two different values), the λ values were determined from measurements along two axes (x - and y -axis, i.e., along and across the fibers). Each data point (mean + S.E.M.) was calculated from α and λ values recorded at 5 min intervals. The number of experiments was 9 (x -axis) or 5 (y -axis) for the application of 50 mM K^+ and 6 (both axes) for the application of hypotonic solution. Isoconcentration plots were constructed from the diffusion values recorded at points a, b, c, d, e, and f, as described for Figure 2. Note the change from anisotropic diffusion (ellipses), under control conditions and during the application of 50 mM K^+ or H-40, to isotropic diffusion (circles) after reperfusion with isotonic, 3 mM K^+ ACF.

Mechanisms of K^+ -Evoked Changes in ECS Diffusion Parameters

The key mechanisms of glial K^+ accumulation and swelling in the presence of high potassium levels include carrier-mediated KCl - $NaCl$ uptake and Donnan-mediated KCl fluxes (Kimelberg and Frangakis, 1985; Ballanyi et al., 1987; Walz, 1992). We therefore examined the effect of inhibitors of astrocyte swelling on the K^+ -evoked changes in ECS diffusion parameters, namely, of Cl^- -free solution, application of furosemide (Na - K - $2Cl$ and Cl/HCO_3^- transport inhibitor), bumetanide (Na - K - $2Cl$ co-transport inhibitor) (Kimelberg et al., 1990; Olson et al., 1995), and block of K^+ channels by Ba^{++} (Walz and Mukerji, 1988).

In all age groups, the decrease in α and increase in λ evoked by the application of 50 mM K^+ were blocked in Cl^- -free solution (Fig. 5A). Furosemide (2 mM), when applied 20 min prior to and together with 50 mM K^+ , slowed down the K^+ -evoked decrease in α , but had no effect on the increase of λ . The decrease in α took about 10 min in ACF (see Fig. 3B) as compared to at least 45 min in furosemide (Fig. 5B). Bumetanide (0.1 mM) had a very similar effect as furosemide (Fig. 5C). After washing out the 50 mM K^+ that was applied with furosemide or bumetanide, there was a slow and incomplete recovery with no sign of Phase II, III, or IV (compare Fig. 3B and Fig. 5 B,C). The application of 5 mM Ba^{++} had no effect on the time course or amplitude of K^+ -evoked changes in α and λ (not shown).

To exclude the possibility that application of potassium resulted in an increase in synaptic activity due to activation of neuronal receptors, and in a release of

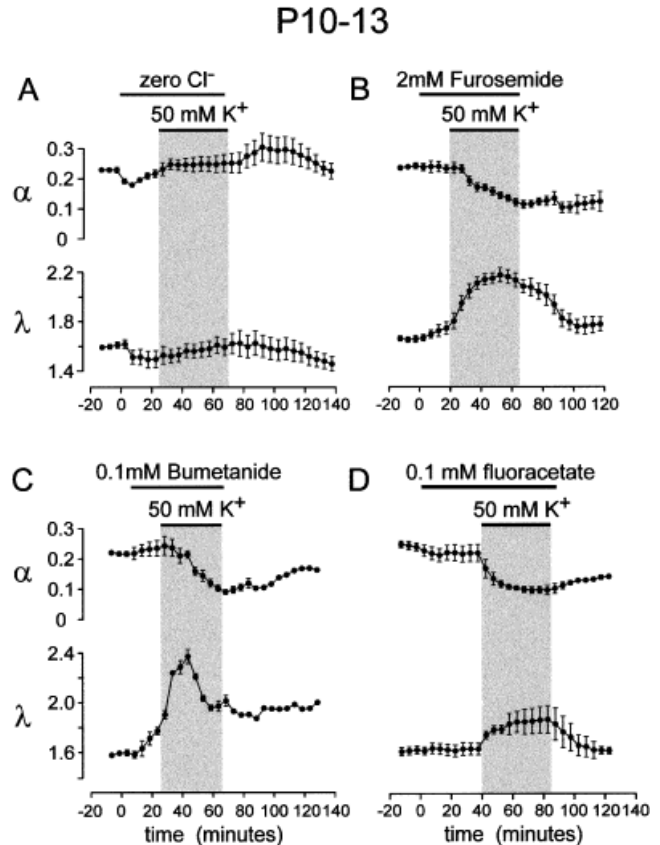


Fig. 5. The effects of Cl^- -free solution (A), furosemide (B), bumetanide (C) and fluoroacetate (D) on potassium-evoked changes in α and λ . Each data point (mean + S.E.M.) was calculated from α and λ values recorded at 5 min intervals from three (A), seven (B), three (C), and five (D) experiments. The blocking agents were applied both 20–25 (A,B,C) or 40 (D) min before and also during perfusion with 50 mM K^+ . Note that potassium-evoked changes were blocked in Cl^- -free solution; furosemide and bumetanide extended Phase I, while Phases II, III, and IV were blocked (for description of Phase I–IV see the legend to Fig. 3).

glutamate, which may also cause cell swelling, we studied the effect of 50 mM K^+ in a Ca^{++} -free solution (with 1 mM EGTA added) and in a solution with 20 mM Mg^{++} . The typical decrease in α and increase in λ evoked by the application of 50 mM K^+ were not significantly altered by a prior (20 min) and concomitant application of high Mg^{++} or Ca^{++} -free solution (not shown).

To further evaluate the role of glia in the observed changes in ECS diffusion parameters evoked by high K^+ , we studied the effect of fluoroacetate, an inhibitor of the glial tricarboxylic acid cycle (Swanson and Graham, 1994; Fonnum et al., 1997). Fluoroacetate, when applied prior to 50 mM K^+ at a relatively low concentration of 10^{-4} M (Fonnum et al., 1997), did not significantly affect α and λ values. When applied with 50 mM K^+ , it had no effect on the K^+ -evoked decrease of α , but the increase of λ was smaller (about 1.87, compare Figs. 3B and 5D). Fluoroacetate blocked Phase II and the recovery of α in ACF (Phase III and IV). Interestingly, there was a complete recovery of λ , again suggesting that changes in α and λ can occur independently and may have different origins. Our results show that in low concentration, fluoroacetate did not affect K^+ -evoked glial swelling but impaired recovery phases related to cell shrinkage.

K⁺- and Hypotonic Stress-Evoked Changes in Astrocyte and Oligodendrocyte Morphology

Our data show that elevated K⁺ or hypotonic stress did not always lead to a concomitant decrease in ECS volume and an increase in tortuosity. This was only the case in the initial phase of cell swelling. When α returned towards control values, apparently due to cell shrinkage, and when it overshoot control values, tortuosity was still increased, presumably due to changes in glial morphology, proliferation, hypertrophy, and rearrangement of fine glial processes. To test this hypothesis we studied the effect of K⁺- and H-40 application on astrocyte and oligodendrocyte morphology.

The increase in α (ECS overshoot) and, particularly, the persistent increase in λ seen in spinal cords superfused for 45 min with 50 mM K⁺ (Phase IV) were accompanied by a massive increase in GFAP staining; astrocytes revealed thicker processes and more dense somata than those in spinal cords superfused with normal ACF (Fig. 6A,B,E,F). A smaller but still distinct increase in GFAP staining was also observed after superfusion with H-40 (Fig. 6C,D). In addition to swollen and hypertrophied glial processes, diffusion barriers can also be formed by changes in the extracellular matrix. More pronounced staining for proteoglycans has been found during astrogliosis (Bignami and Dahl, 1995), and recently we found that levels of chondroitin sulfate proteoglycans (CSPG) are higher in the extracellular space of gliotic tissue in cortical grafts examined 1–6 months post-transplantation (Harvey et al., 1997). Staining with CS-56 monoclonal antibody revealed that the overall level of extracellular CSPG in spinal cords superfused at first with 50 mM K⁺ and then 60–100 min with ACF was not appreciably higher than that seen in spinal cords incubated only in physiological ACF; there were occasional darker spots only. Moreover, CSPG formed characteristic coats around motoneurons, called perineuronal nets (Fig. 7A). These fine coats around motoneurons disappeared after K⁺ application and were replaced by darker CSPG spots, probably due to the condensation of the CSPG coats around the shrunken cells (Fig. 7B). Cresyl violet staining revealed that motoneuronal bodies were elongated and shrunken (Fig. 7C,D).

In white matter, oligodendrocyte staining by Rip revealed that after 45 min superfusion with H-40, white matter was broader by 15–25% with larger spacing between the myelinated axons and overall staining by Rip was reduced (Fig. 8A,B). No significant increase in WM thickness was found after superfusion with 50 mM K⁺ (not shown). After superfusion with either 50 mM K⁺ or H-40 and then 60–100 min with ACF, i.e., during the period when α returned to control values, there was still an increase in λ and a loss of anisotropy (see Fig. 4); GFAP staining revealed the loss of the typical radial organization of astroglial processes in WM (ventral funiculus) (Fig. 8C,D,E).

We conclude that astrogliosis and the observed changes in astrocyte morphology following the application of high K⁺ or hypotonic stress may result in long-term or “persistent” changes in ECS diffusion

barriers, in our measurements manifested by a decrease in the ADC of TMA⁺, i.e., an increase in tortuosity that is independent of ECS volume changes.

DISCUSSION Mechanisms of ECS Volume and Tortuosity Changes

This study shows that the two important diffusion parameters, ECS volume and tortuosity, change during glial swelling evoked by a potassium elevation as well as during hypotonic stress and, importantly, that these two variables change independently. Similar to results reported in turtle cerebellum, we have found relatively small changes in overall tissue volume during and after hypoosmotic stress (about 2%) (Križaj et al., 1996) and no changes at all after 50 mM K⁺, showing that the observed changes in ECS volume are due initially to cell swelling and later to cell shrinkage. While cells quickly regulate their volume, the structure and thickness of fine glial processes can remain altered for hours.

In the CNS, swelling induced by high potassium is confined mainly to astrocytes (for review see Kimelberg and Frangakis, 1985; Kimelberg and Ransom, 1986). Since the application of furosemide and bumetanide (but not of Ba⁺⁺) substantially slowed down the changes in ECS diffusion parameters evoked by high potassium, and since these changes were blocked in Cl⁻-free medium, it is likely that the changes in Phase I are due to cell swelling resulting from a net KCl uptake via Na-K-2Cl cotransport and concomitant water influx into astrocytes as well as a change in the Donnan equilibrium (Walz and Hinks, 1985). Another mechanism which could affect K⁺ distribution by glia is potassium spatial buffering (Orkand et al., 1966). This mechanism is, however, unlikely to play an important role in the observed changes, since the rise in extracellular K⁺ concentration was rather uniform in the whole spinal cord, and it should not be affected by the K_{IR} channel blocker, Ba⁺⁺.

In addition to swelling produced by Donnan forces neuronal swelling could also be evoked by K⁺ as a consequence of an increase in excitability and transmitter release produced by depolarization. This swelling would be attributable to a NaCl influx or enhanced metabolic processes, which increase intracellular osmolarity (Dietzel et al., 1989). However Serve et al. (1988) described a shrinkage of neuronal somata during their stimulation. During pathological states such as ischemia, the swelling of astrocytic perikarya and processes is typical; in contrast, swelling in neurons is small or absent, irregular, and occurs later (Jenkins et al., 1984). Glutamate receptor activation also results in astrocyte swelling (Chan et al., 1990; Hannson and Rönnbäck, 1994). However, in our study, K⁺-evoked swelling was not affected by a lack of extracellular Ca⁺⁺ or the blocking of Ca⁺⁺ channels by 20 mM Mg⁺⁺. Synaptically-transmitted responses were also reported to be increased during hypotonic exposure and depressed thereafter (Andrew, 1991; Ballyk et al., 1991; Hester et al., 1993; Chebabo et al., 1995a), possibly due to changes in the width of the synaptic clefts.

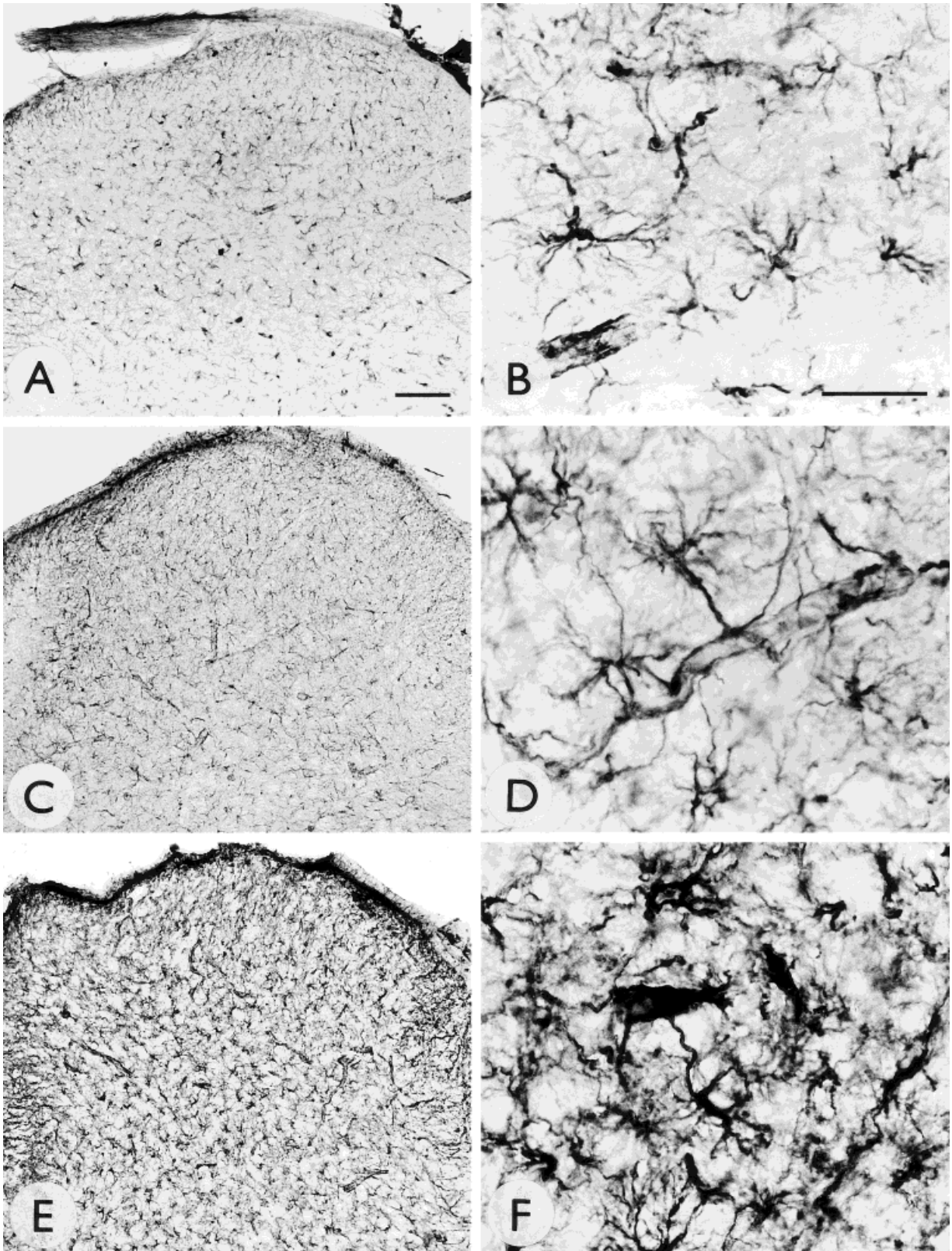


Fig. 6. Astrocytes stained for GFAP in transversal sections of P13 dorsal spinal horns. **A,B:** Isolated spinal cord incubated for 145 min in ACF. **C,D:** Spinal cord superfused for 40 min with hypotonic solution followed by 100 min superfusion with control ACF. **E,F:** Spinal cord

superfused for 45 min with 50 mM K^+ followed by 100 min superfusion with control ACF. Note the increase in GFAP immunoreactivity and the densely stained, thick processes in C-F. Scale bar: A: 100 μ m; (A,C,E), in B = 50 μ m (B,D,F).

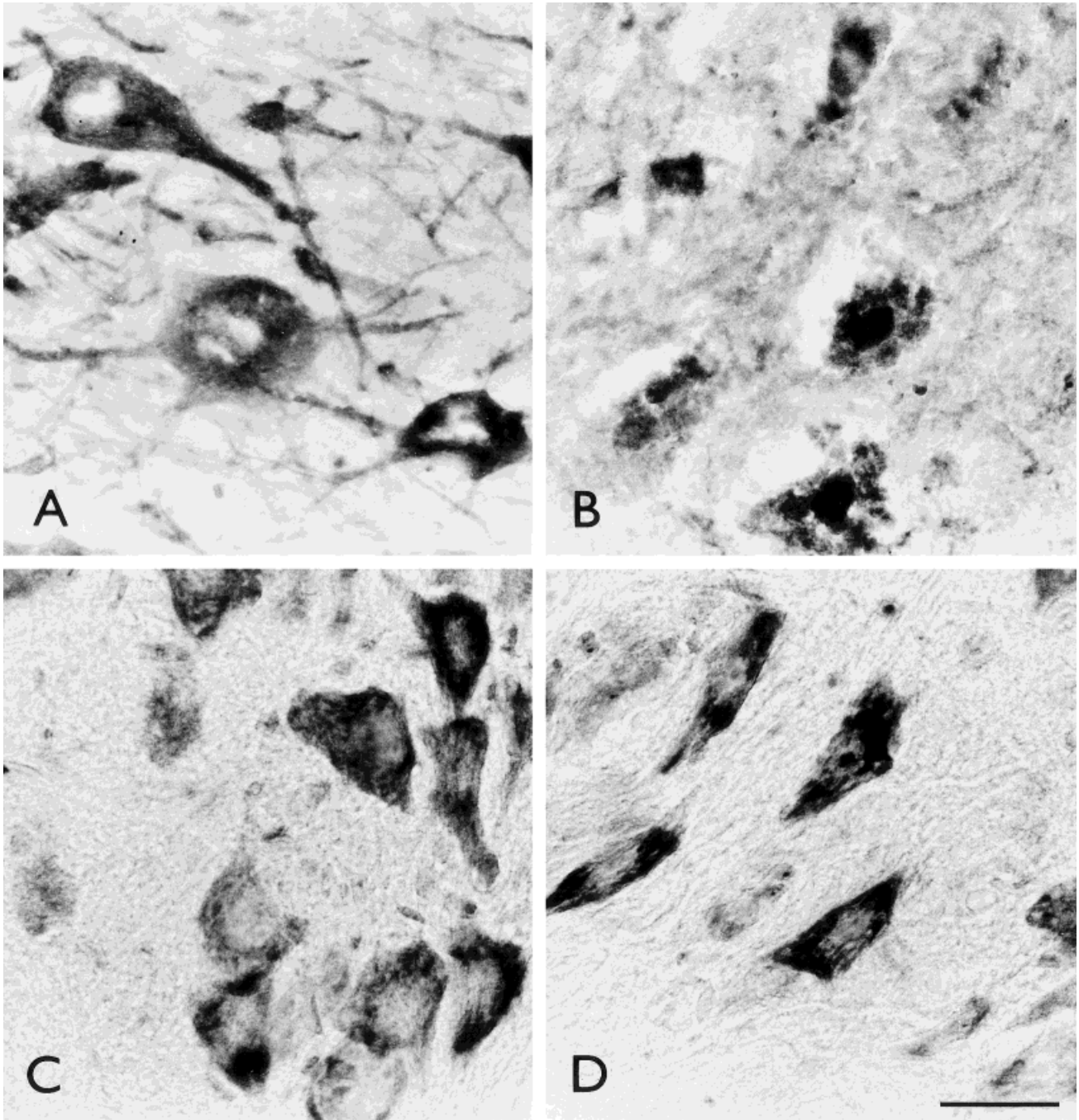


Fig. 7. **A,B:** Distribution of chondroitin sulfate proteoglycan (CSPG) as revealed by CS-56 antibody. Note that in control spinal cord (A), CSPG forms perineural nets around motoneurons, while after perfusion with 50 mM K⁺ and washout for 100 min in ACF (B), CSPG around motoneurons was condensed into dark spots. Deposits of CSPG

can also be seen in the ECS. **C,D:** Cresyl violet Nissl staining in control spinal cord (C) and in spinal cord after perfusion with 50 mM K⁺, showing elongated and shrunken cell bodies of motoneurons (D). Scale bar = 50 μ m (A–D).

The diffusion of a particular substance in a tissue apparently depends on both diffusion parameters; it decreases not only with a decrease in the ECS volume fraction (pore size), but also with an increase in tortuosity resulting from additional diffusion barriers. In our experiments, we found tortuosity increase to be independent of ECS volume decrease. There was a significant tortuosity increase evoked by the application of 10 and 20 mM K⁺, while the changes in ECS volume were

insignificant (Fig. 1). The second rise in λ was delayed, i.e., it started many minutes after the application of hypotonic solution or high K⁺, during the period of astrogliosis when the cells were shrunken (Fig. 8C,D) and ECS volume fraction increased. It may well be that when fine cell processes swell, or when the processes become thicker as is the case during astrogliosis, the overall decrease in ECS may be small but additional diffusion barriers can still be formed. It has been

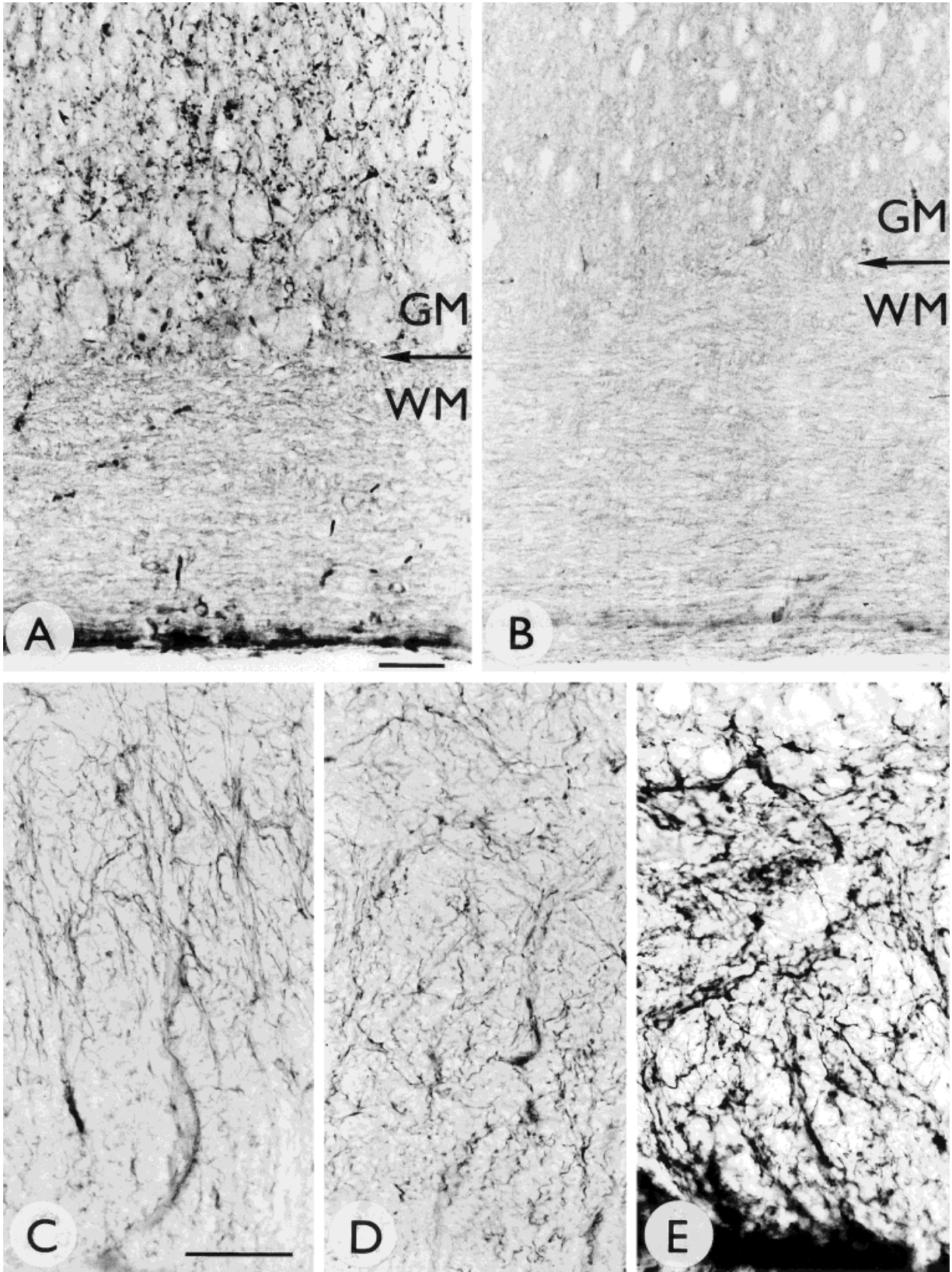


Fig. 8. Longitudinal sections of P13 spinal cords stained with Rip antibody (A,B). **A:** Control spinal cord with densely stained oligodendrocytic structures in both white and gray matter. **B:** In spinal cord after 45 min superfusion with hypotonic solution the white matter is wider than in control spinal cord, and the Rip staining is less dense in both gray and white matter. **C-E:** Transversal sections of ventral horn

white matter stained for GFAP. The typical radial organization of astroglial processes in control spinal cord (C) disappears after the application of hypotonic solution (D) or 50 mM K^+ (E). Arrow indicates the border between gray (GM) and white matter (WM). Scale bar: in A = 50 μ m (A,B), in C = 50 μ m (C-E).

previously suggested that glial processes and neuronal dendrites swell more than glial and neuronal somata (Van Harreveld and Khattab, 1967; Kimelberg et al., 1992; Andrew and MacVicar, 1994). Astroglial processes may also result in the increased production or condensation of extracellular matrix and therefore in an increase in diffusion barriers. However, we have not found increased staining for ECS chondroitin sulfate proteoglycans, although there was a condensation of the perineuronal nets (Fig. 8A,B). Thus, the exact nature of the tortuosity increase during astroglial processes is still not clear.

Cell swelling and post-hypotonic cell shrinkage, resulting in changes in ECS volume have also been reported in rat hippocampal slices (Chebabo et al., 1995b). However, this study did not take into account tortuosity changes and only reported the relative values of ECS volume changes. When one uses the relative changes in TMA⁺ diffusion curves, measurements of the ECS volume are not accurate. The larger decrease in ECS volume observed in hippocampal slices, using similar hypotonic solutions as in our study (Chebabo et al., 1995b), might therefore be overestimated. Moreover, we recently reported that diffusion in hippocampus is anisotropic (Syková et al., 1997; Mazel et al., 1998), and thus accurate values for the ECS volume fraction in hippocampus cannot be obtained using measurements performed only in one axis.

Our study also shows that the cellular swelling evoked by hypotonic solution and by high K⁺ have different effects on ECS diffusion parameters. While both lead to about the same decrease in ECS volume, high potassium results in persistent and much greater changes in ECS tortuosity than does hypotonic solution (Table 2). We suggest that this increase in tortuosity is related to astroglial processes. Indeed, we found much greater astroglial processes in response to high K⁺ than to hypotonic solution. It has been previously reported that exposure to high K⁺ results in the progressive appearance of cell processes immunoreactive for GFAP (Canady et al., 1990; Kraig et al., 1991; Del Bigio et al., 1994; Del Cerro et al., 1996).

Studies of ECS Diffusion Parameters In Vivo, In Situ and in Brain Slices

The degree to which swelling of mammalian nerve cells affects the diffusion of neuroactive substances in the ECS has not been previously determined in situ. To the best of our knowledge, the only in situ study that examined ECS diffusion parameters was done in the isolated turtle cerebellum following osmotic changes, and no study has described the changes evoked by a potassium increase. While the large changes in osmolarity used in these studies are only rarely observed, even during severe pathological states, transient and reversible increases in extracellular K⁺ concentration to 10, 20, and, under pathological conditions, to 50–70 mM are very common (Syková, 1983, 1992, 1997).

Our study revealed that changes in ECS diffusion parameters are somewhat different from those in slice preparations 250–400 µm thick. In this study we found

much larger changes in tortuosity than those seen in slices (for review see Syková, 1997; Nicholson and Syková, 1998), but similar changes in ECS volume fraction (Andrew and MacVicar, 1994; Chebabo et al., 1995b). The values in isolated spinal cord closely resemble those in spinal cord in vivo during pathological states (an increase of λ above 2.0) (Syková et al., 1994; Voříšek and Syková, 1997b). Similarly, during recovery from anoxia in spinal cord in vivo, α increased and remained elevated above normal values for more than 2 h (Syková et al., 1994), a finding which is in good agreement with the ECS volume overshoot observed in our present study. However, there can also be interspecies or regional differences. In the isolated turtle cerebellum during the application of hypoosmotic solution, tortuosity increased only from 1.70 to 1.79 (Križaj et al., 1996) and in rat brain slices during anoxia from about 1.6 to 1.75 (Pérez-Pinzon et al., 1995). Križaj et al. (1996) did not observe signs of RVD (see below) in the isolated turtle cerebellum, while it was observed in rat hippocampal slices (Chebabo et al., 1995b). The tortuosity changes seen in mammalian brain slices might be artificially low, presumably due to either the washing out of macromolecules from the extracellular space, reduced swelling of cut cellular processes, or other unknown reasons. Somjen et al. (1993) reported that freshly dissociated hippocampal pyramidal cells, with most of their dendrites lost during cell suspension preparation, do not seem to swell at all. They suggest that the swelling of cells in vivo and in situ is limited to the dendritic tree and glial cells.

ECS Diffusion Parameters in White Matter

Diffusion in the ECS may be channeled, that is, more hindered in one direction than in another. This so-called diffusion anisotropy has been described in cerebellum (Rice et al., 1993), hippocampus (Syková et al., 1997; Mazel et al., 1998), and myelinated white matter (Bjelke et al., 1995; Chvátal et al., 1997; Prokopová et al., 1997; Voříšek and Syková, 1997a). In myelinated white matter, preferential diffusion of TMA⁺ occurs along the myelinated axons, i.e., a much higher value of tortuosity is seen across the myelinated axons (Prokopová et al., 1997; Voříšek and Syková, 1997a). Our study shows that cell swelling leads to an uneven increase in tortuosity along and across the axons and that anisotropy is diminished long after the application of hypotonic solution or high K⁺, presumably due to morphological and structural changes (see Fig. 8C,D,E). Anisotropy, which permits more rapid diffusion in one direction than in another, can thus be lost during and long after pathological states accompanied by cell swelling and astroglial processes. The loss of anisotropy can thus have important consequences for the specificity and efficacy of extrasynaptic transmission.

ECS Diffusion Parameters and Regulatory Volume Decrease (RVD)

Most animal cells regulate their volume after exposure to changes in the osmolarity of their microenviron-

ment (Hoffman and Simonsen, 1989). Astrocytes swell rapidly in hypotonic conditions and then show RVD over the course of 15–30 min, due to a net reduction in the total intracellular osmolyte content (Kimelberg and Frangakis, 1985; Olson et al., 1986). Several intracellular constituents are lost, including potassium, taurine and other amino acids (Kimelberg et al., 1990; Bender and Norenberg, 1994; Vitarella et al., 1994). Cellular shrinkage apparently results from RVD (Cserr et al., 1991; Strange, 1992; Gullans and Verbalis, 1993). This is in good agreement with our study, since during exposure to either high potassium or hypotonic stress, ECS volume fraction tended to recover and then increase above control values. This regulation of ECS volume was, in our studies, less effective in immature animals (less advanced gliogenesis). It was blocked by a low dose of fluoroacetate, which blocks glial metabolism, suggesting that most of the ECS volume changes are due to swelling and shrinkage of glial cells. Histological studies verified that fluoroacetate led to glial and neuronal damage only after 3–4 h of application (Largo et al., 1996). Although fluoroacetate is primarily affecting astrocytic metabolism, we cannot exclude that within 85 min of its application there was also an effect on neuronal metabolism. To the best of our knowledge, the effect of these gliotoxins on RVD has not yet been studied. The importance of glial swelling is also supported by the fact that cell shrinkage was more pronounced after high K^+ than after hypotonic stress, since glial cells serve to maintain extracellular K^+ homeostasis (for review see Syková, 1992, 1997). Post-hypotonic shrinkage of cells is explained by the loss of solutes from cells during RVD because normal ACF is hypertonic relative to the ion-depleted cytosol. The cell shrinkage when cells are returned to isotonic media after hypotonic stress may have a different mechanism than that responsible for RVD. A Ca^{++} -sensitive mechanism of cell shrinkage in isotonic media may be responsible for the subsequent increase in ECS volume after the application of high K^+ (Fig. 7C,D). It has been shown that an increase in intracellular Ca^{++} in neuroblastoma cells under isotonic conditions produces cell shrinkage (Crowe et al., 1995).

In summary, astrocyte swelling can influence both the size of the ECS volume and the degree of ECS tortuosity around neurons, slowing down diffusion in the ECS and thus modulating neuronal activity and neuron-glia interaction. Recently, there have been a number of reports suggesting the occurrence of 'crosstalk' between distinct synapses or the "spillover" of glutamate (for review see Barbour and Hausser, 1997; Kullman and Asztely, 1998). Transmitters that are released from one synapse can lead to significant activation of high-affinity receptors at neighboring synapses. Crosstalk will, of course, ultimately be dependent on the extracellular space around the synapses, i.e., on intersynaptic geometry and diffusion parameters. Finally, since the diffusion of neuroactive substances is the underlying mechanism of extrasynaptic transmission, not only astroglial but also more subtle

changes in astrocyte morphology may produce transient or persistent changes in signal transmission.

ACKNOWLEDGMENTS

We thank Dr. I. Hájek for his contribution in the initial phase of the measurement of total water content.

REFERENCES

- Agnati LF, Zoli M, Stromberg I, Fuxe K. 1995. Intercellular communication in the brain: Wiring versus volume transmission. *Neuroscience* 69:711–726.
- Andrew RD. 1991. Seizure and acute osmotic change: clinical and neurophysiological aspects. *J Neurol Sci* 101:7–18.
- Andrew RD, MacVicar BA. 1994. Imaging cell volume changes and neuronal excitation in the hippocampal slice. *Neuroscience* 62:371–383.
- Ballanyi K, Grafe P, ten Bruggencate G. 1987. Ion activities and potassium uptake mechanisms of glial cells in guinea-pig olfactory cortex slices. *J Physiol (Lond)* 382:1590–1740.
- Ballyk BA, Quackenbush SJ, Andrew RD. 1991. Osmotic effects on the CA1 neuronal population in hippocampal slices with special reference to glucose. *J Neurophysiol* 65:1055–1066.
- Barbour B, Hausser M. 1997. Intersynaptic diffusion of neurotransmitter. *Trends Neurosci* 20:377–384.
- Bender AS, Norenberg MD. 1994. Calcium dependence of hypoosmotically induced potassium release in culture astrocytes. *J Neurosci* 14:4237–4243.
- Benveniste H, Hedlund LW, Johnson GA. 1992. Mechanism of detection of acute cerebral ischemia in rats by diffusion-weighted magnetic resonance microscopy. *Stroke* 23:746–754.
- Bignami A, Dahl D. 1995. Gliosis. In: *Neuroglia*. Kettenmann H, Ransom BR, eds. New York: Oxford University Press. p. 843–858.
- Bjelke B, England R, Nicholson C, Rice ME, Lindberg J, Zoli M, Agnati LF, Fuxe K. 1995. Long distance pathways of diffusion for dextran along fibre bundles in brain. Relevance for volume transmission. *Neuroreport* 6:1005–1009.
- Canady KS, Ali-Osman F, Rubel EW. 1990. Extracellular potassium influences DNA and protein synthesis and glial fibrillary acidic protein expression in cultured glial cells. *Glia* 3:368–374.
- Chan PH, Chu L, Chen S. 1990. Effects of MK-801 on glutamate-induced swelling of astrocytes in primary cell culture. *J Neurosci Res* 25:87–93.
- Chebabo SR, Hester MA, Aitken PG, Somjen GG. 1995a. Hypotonic exposure enhances synaptic transmission and triggers spreading depression in rat hippocampal tissue slices. *Brain Res* 695:203–216.
- Chebabo SR, Hester MA, Jing J, Aitken PG, Somjen GG. 1995b. Interstitial space, electrical resistance and ion concentrations during hypotonia of rat hippocampal slices. *J Physiol (Lond)* 487:685–697.
- Chvátal A, Berger T, Vorišek I, Orkand RK, Kettenmann H, Syková E. 1997. Changes in glial K^+ currents with decreased extracellular volume in developing rat white matter. *J Neurosci Res* 49:98–106.
- Crowe WE, Altamirano J, Heurto L, Alvarez-Leefmans FJ. 1995. Volume changes in single N1E-115 neuroblastoma cells measured with a fluorescent probe. *Neuroscience* 69:283–296.
- Cserr HF, De Pasquale M, Nicholson C, Patlak C, Pettigrew KD, Rice ME. 1991. Extracellular volume decreases while cell volume is maintained by ion uptake in rat brain during acute hypernatremia. *J Physiol (Lond)* 442:277–295.
- Del Bigio MR, Omara F, Fedoroff S. 1994. Astrocyte proliferation in culture following exposure to potassium ion. *Neuroreport* 5:639–641.
- Del Cerro S, Garcia-Estrada J, Garcia-Segura LM. 1996. Neurosteroids modulate the reaction of astroglia to high extracellular potassium levels. *Glia* 18:293–305.
- Dietzel I, Heinemann U, Lux HD. 1989. Relations between slow extracellular potential changes, glial potassium buffering, and electrolyte and cellular volume changes during neuronal hyperactivity in cat brain. *Glia* 2:25–44.
- Fonnum F, Johnsen A, Hassel B. 1997. Use of fluorocitrate and fluoroacetate in the study of brain metabolism. *Glia* 21:106–113.
- Friedman B, Hockfield S, Black JA, Woodruff KA, Waxman SG. 1989. In situ demonstration of mature oligodendrocytes and their processes: an immunocytochemical study with a new monoclonal antibody. *Rip*. *Glia* 2:380–390.
- Fuxe K, Agnati LF. 1991. *Volume Transmission in the Brain: Novel Mechanisms for Neural Transmission*. New York: Raven Press.

- Gullans SR, Verbalis JG. 1993. Control of brain volume during hyperosmolar and hypoosmolar conditions. *Annu Rev Med* 44:289–301.
- Hansson E, Rönnbäck L. 1994. Astroglial modulation of synaptic transmission. *Perspec Dev Neurobiol* 2:217–223.
- Harvey AR, Kendall CL, Syková E. 1997. The status and organization of astrocytes, oligodendroglia and microglia in grafts of fetal rat cerebral cortex. *Neurosci Lett* 227:58–62.
- Hester MA, Aitken PG, Somjen GG. 1993. Hypotonic environment enhances synaptic potentials in hippocampal tissue slices. *Soc Neurosci Abstr* 19:715.
- Hoffman EK, Simonsen LO. 1989. Membrane mechanisms in volume and pH regulation in vertebrate cells. *Physiol Rev* 69:315–382.
- Holthoff K, Witte OW. 1996. Intrinsic optical signals in rat neocortical slices measured with near-infrared dark-field microscopy reveal changes in extracellular space. *J Neurosci* 16:2740–2749.
- Jenkins LW, Becker DP, Coburn TH. 1984. A quantitative analysis of glial swelling and ischemic neuronal injury following complete cerebral ischemia. In: *Recent Progress in the Study and Therapy of Brain Edema*. Go KG, Baethmann A, eds. New York: Plenum p. 523–537.
- Kimelberg HK. 1991. Swelling and volume control in brain astroglial cells. In: *Advances in Comparative and Environmental Physiology*. Gilles R, et al., eds. Berlin, Heidelberg: Springer-Verlag p. 81–117.
- Kimelberg HK, Frangakis MV. 1985. Furosemide- and bumetanide-sensitive ion transport and volume control in primary astrocyte cultures from rat brain. *Brain Res* 361:125–134.
- Kimelberg HK, Goderie SK, Higman S, Pang S, Waniewski RA. 1990. Swelling-induced release of glutamate aspartate and taurine from astrocyte cultures. *J Neurosci* 10:1583–1591.
- Kimelberg HK, Ransom BR. 1986. Physiological and pathological aspects of astrocyte swelling. In: *Astrocytes: Cell Biology and Pathology of Astrocytes*. Federoff S, Vernadakis A, eds. New York Academic Press p. 129–166.
- Kimelberg HK, Sankar P, O'Connor ER, Jalonon T, Goderie SK. 1992. Functional consequences of astrocyte swelling. *Prog Brain Res* 94:57–68.
- Kraig RP, Dong L, Thisted R, Jaeger CB. 1991. Spreading depression increases immunohistochemical staining of glial fibrillary acidic protein. *J Neurosci* 11:2187–2198.
- Krizaj D, Rice ME, Wardle RA, Nicholson C. 1996. Water compartmentalization and extracellular tortuosity after osmotic changes in cerebellum of *Trachemys scripta*. *J Physiol (Lond)* 492:887–896.
- Kullmann DM, Asztely F. 1998. Extrasynaptic glutamate spillover in the hippocampus: evidence and implications. *Trends Neurosci* 21:8–14.
- Largo C, Cuevas P, Somjen GG, Martin del Rio R, Herreras O. 1996. The effect of depressing glial function in rat brain *in situ* on ion homeostasis, synaptic transmission, and neuron survival. *J Neurosci* 16:1219–1229.
- Latour LL, Svoboda K, Mitra PP, Sotak CH. 1994. Time-dependent diffusion of water in a biological model system. *Proc Natl Acad Sci USA* 91:1229–1233.
- Lehmenkühler A, Syková E, Svoboda J, Zilles K, Nicholson C. 1993. Extracellular space parameters in the rat neocortex and subcortical white matter during postnatal development determined by diffusion analysis. *Neuroscience* 55:339–351.
- Lipton P. 1973. Effects of membrane depolarization on light scattering by cerebral cortical slices. *J Physiol (Lond)* 231:365–383.
- MacVicar BA, Hochman D. 1991. Imaging of synaptically evoked intrinsic optical signals in hippocampal slices. *J Neurosci* 11:1458–1469.
- Mazel T, Šimonová Z, Syková E. 1998. Diffusion heterogeneity an anisotropy in rat hippocampus. *Neuroreport* 9:1299–1304.
- Nicholson C, Phillips JM. 1981. Ion diffusion modified tortuosity and volume fraction in the extracellular microenvironment of the rat cerebellum. *J Physiol (Lond)* 321:225–257.
- Nicholson C, Rice ME. 1991. Diffusion of ions and transmitters in the brain cell microenvironment. In: *Volume Transmission in the Brain, Novel Mechanisms for Neural Transmission*. Fuxe K, Agnati LF, eds. New York: Raven Press. p. 279–294.
- Nicholson C, Syková E. 1998. Extracellular space structure revealed by diffusion analysis. *Trends Neurosci* 21:207–215.
- Norris DG, Niendorf T, Leibfritz D. 1994. Healthy and infarcted brain tissues studied at short diffusion times: the origins of apparent restriction and the reduction in apparent diffusion coefficient. *NMR Biomed* 7:304–310.
- Olson JE, Alexander C, Feller DA, Clayman ML, Ramnath EM. 1995. Hypoosmotic volume regulation of astrocytes in elevated extracellular potassium. *J Neurosci Res* 40:333–342.
- Olson JE, Sankar R, Holtzman D, James A, Fleischhacker D. 1986. Energy dependent volume regulation in primary cultured cerebral astrocytes. *J Cell Physiol* 128:209–215.
- Orkand RK, Nicholls JG, Kuffler SW. 1966. The effect of nerve impulses on the membrane potential of glial cells in the central nervous system of amphibia. *J Neurophysiol* 29:788–806.
- Pasantes-Morales H, Murray RA, Lilja L, Morán J. 1994. Regulatory volume decrease in cultured astrocytes I. Potassium- and chloride-activated permeability. *Am J Physiol* 266:C165–C171.
- Pasantes-Morales H, Schousboe A. 1988. Volume regulation in astrocytes: a role for taurine as osmoeffector. *J Neurosci Res* 20:505–509.
- Pérez-Pinzo MA, Tao L, Nicholson C. 1995. Extracellular potassium, volume fraction, and tortuosity in rat hippocampal CA1, CA3, and cortical slices during ischemia. *J Neurophysiol* 74:565–573.
- Prokopová Š, Vargová L, Syková E. 1997. Heterogeneous and anisotropic diffusion in the developing rat spinal cord. *Neuroreport* 8:3527–3532.
- Ransom BR, Yamate CL, Connors BW. 1985. Activity dependent shrinkage of extracellular space in rat optic nerve: A developmental study. *J Neurosci* 5:532–535.
- Rice ME, Okada YC, Nicholson C. 1993. Anisotropic and heterogeneous diffusion in the turtle cerebellum: Implications for volume transmission. *J Neurophysiol* 70:2035–2044.
- Serve G, Endres W, Grafe P. 1988. Continuous electrophysiological measurements of changes in cell volume of motoneurons in the isolated frog spinal cord. *Pflügers Arch* 411:410–415.
- Šimonová Z, Svoboda J, Orkand R, Bernard CCA, Lassmann H, Syková E. 1996. Changes of extracellular space volume and tortuosity in the spinal cord of Lewis rats with experimental autoimmune encephalomyelitis. *Physiol Res* 45:11–22.
- Somjen GG, Faas GC, Vreugdenhil M, Wadman WJ. 1993. Channel shutdown: a response of hippocampal neurons to adverse environments. *Brain Res* 632:180–194.
- Strange K. 1992. Regulation of solute and water balance and cell volume in the central nervous system. *J Am Soc Nephrol* 3:12–27.
- Svoboda J, Syková E. 1991. Extracellular space volume changes in the rat spinal cord produced by nerve stimulation and peripheral injury. *Brain Res* 560:216–224.
- Swanson RA, Graham SH. 1994. Fluorocitrate and fluoroacetate effects on astrocyte metabolism *in vitro*. *Brain Res* 664:94–100.
- Syková E. 1983. Extracellular K⁺ accumulation in the central nervous system. *Prog Biophys Molec Biol* 42:135–189.
- Syková E. 1987. Modulation of spinal cord transmission by changes in extracellular K⁺ activity and extracellular volume. *Can J Physiol Pharmacol* 65:1058–1066.
- Syková E. 1992. Ionic and Volume Changes in the Microenvironment of Nerve and Receptor Cells. Heidelberg: Springer-Verlag.
- Syková E. 1997. The extracellular space in the CNS: Its regulation, volume and geometry in normal and pathological neuronal function. *Neuroscientist* 3:28–41.
- Syková E, Mazel T, Roitbak T, Voříšek I. 1997. Heterogeneous and anisotropic diffusion in the rat brain during development and ageing. *Soc Neurosci Abstr* 23:587.
- Syková E, Svoboda J, Polák J, Chvátal A. 1994. Extracellular volume fraction and diffusion characteristics during progressive ischemia and terminal anoxia in the spinal cord of the rat. *J Cereb Blood Flow Metab* 14:301–311.
- Syková E, Svoboda J, Šimonová Z, Lehmenkühler A, Lassmann H. 1996. X-irradiation-induced changes in the diffusion parameters of the developing rat brain. *Neurosci* 70:597–612.
- Syková E, Vargová L, Šimonová Z, Nicholson C. 1995. Effects of K⁺, hypotonic solution, glutamate, AMPA and NMDA on the diffusion parameters in isolated rat spinal cord during development. *Soc Neurosci Abstr* 21:222.
- Van der Toorn A, Syková E, Dijkhuizen RM, Voříšek I, Vargová L, Skobisová E, van Lookeren Campagne M, Reese T, Nicolay K. 1996. Dynamic changes in water ADC, energy metabolism, extracellular space volume, and tortuosity in neonatal rat brain during global ischemia. *Magn Reson Med* 36:52–60.
- Van Harreveld A, Khattab FI. 1967. Changes in cortical extracellular space during spreading depression investigated with the electron microscope. *J Neurophysiol* 30:911–929.
- Vitarella D, DiRisio DJ, Kimelberg HK, Aschner M. 1994. Potassium and taurine release are highly correlated with regulatory volume decrease in neonatal primary rat astrocyte cultures. *J Neurochem* 63:1143–1149.
- Voříšek I, Syková E. 1997a. Evolution of anisotropic diffusion in the developing rat corpus callosum. *J Neurophysiol* 78:912–919.
- Voříšek I, Syková E. 1997b. Ischemia-induced changes in the extracellular space diffusion parameters, K⁺ and pH in the developing rat cortex and corpus callosum. *J Cereb Blood Flow Metab* 17:191–203.
- Walz W. 1992. Mechanism of rapid K⁺-induced swelling of mouse astrocytes. *Neurosci Lett* 135:243–246.
- Walz W, Hinks EC. 1985. Carrier-mediated KCl accumulation accompanied by water movements is involved in the control of physiological K⁺ levels by astrocytes. *Brain Res* 343:44–51.
- Walz W, Mukerji S. 1988. KCl movements during potassium-induced cytotoxic swelling of cultured astrocytes. *Exp Neurol* 99:17–29.